Design of SMA Actuator Based Access Device for Transanal Endoscopic Microsurgery

Hongyan Luo[1,2,*], Eric Abel[2], Alan Slade[2], Zhigang Wang[2] and Robert Steele[3]

[1]*Bioengineering College, Chongqing University, Chongqing 400044, P.R. China;* [2]*Division of Mechanical Enginering & Mechatronics, University of Dundee, Dundee DD1 4HN, UK;* [3]*Department of Surgery & Molecular Oncology, Ninewells Hospital & Medical School, University of Dundee, Dundee DD1 9SY, UK*

Abstract: An access device using a combination of a compression coil spring made of NiTi shape memory alloy (SMA) and NiTi superelastic strips has been developed. Particular consideration is given to the application of the concept in transanal endocopic microsurgery (TEM), but it could be used in other procedures where tissue expansion is required. In TEM, it could realize the gasless dilation of the rectum with safety and reliability, and facilitate surgeons to perform TEM. The theoretical design procedure to determine the specifications of the NiTi SMA spring and superelastic components is established. The feasibility and the possible problems associated with this application are discussed generally.

Keywords: Transanal endoscopic microsurgery, Access device, NiTi compression spring, NiTi superelastic strips.

1. INTRODUCTION

Transanal endoscopic microsurgery (TEM) is a mimimal access surgical procedure, which incorporates a device (rectal tube or other access device) to access the rectum, a stereoscopic telescope for viewing, specially designed surgical instruments and a working insert platform with channels for their entrance to perform surgery in rectum through anus. A series of favourable clinical outcomes have proved the clinical success of the method for the treatment of rectal adenomas and selected early rectal cancers [1-4]. However, the use of gas insufflation with carbon dioxide for rectum dilation to expose the surgical field in the original TEM [5] and the resulting practical difficulties such as the need for a good seal to be formed to prevent escape of the gas have mitigated against TEM becoming a popular procedure. These practical difficulties include forming and maintaining effective seals between the access device and the anus and between the surgical instruments and the device at the instrument channels. There are also risks of contamination of the peritoneal cavity by the escaping gas, and especially the risk of dissemination of tumour cells by CO_2 insufflation [6,7].

In recent years, several gasless methods based on the mechanical actuation to expand rectum have been reported by various research groups. These designs, however, either only allow small expansion/exposure of the rectum with the collapse of the rectum beyond the end of the access device, which may obscure the view of the proximal resection margin of tumour [8-10], or they involve the manual control of rectum expansion by adjusting a screw, which might not be very sensitive and could carry the risk of mechanically perforating the rectal wall if the access device is moved too forcibly [11].

*Address correspondence to this author at the Bioengineering College, Chongqing University, Chongqing 400044, P.R. China; Tel/Fax: 0086-23-65111931; E-mail: hongyanzi@gmail.com

In view of these deficiencies, the potential for using NiTi shape memory alloy (SMA) to realize the gasless dilation of the rectum in an electrically controllable way and to provide the adequate exposure of operation site for enhanced safety and reliability has been investigated. We have investigated a two-way shape memory expansion device [12], but two-way training to achieve exact and reliable hot and cold shapes could not be achieved adequately. The use of a SMA spring to activate an expanding cage made from elastic spring strips has also been reported [13]. However, it was not examined in detail.

SMA is a functional material with the ability to recover its predefined shape fully by heating (shape memory effect) or by unloading (superelasticity). Moreover, these properties mean that SMA can also act as an actuator to perform work against a load by implementing a thermal control procedure. These effects arise from the diffusionless phase transformation between low-temperature martensite and high-temperature austenite, which is characterized by four transformation temperatures: martensite start temperature (M_s), martensite finish temperature (M_f), austenite start temperature (A_s) and austenite finish temperature (A_f). Due to a larger recoverable strain than other elastic metals, good corrosion resistance and good biocompatibility, NiTi SMA has advantages over other actuating mechanisms for medical device applications. Furthermore, superelastic NiTi SMA featured by extremely high elasticity and analogous mechanical behaviour to that of the biological materials can even enhance durability during service and improve the surgical intervention with less tissue damage [14,15]. Therefore, replacing the material of the expanding cage in the previous design [13] with superelastic NiTi SMA is considered in our study. This paper presents the design issues and feasibility of a combined shape memory and superelastic access device based on a NiTi compression spring and NiTi superelastic strips, focusing on the TEM access method.

1875-1814/10

2. STRUCTURE AND OPERATING MECHANISM

The structure of the proposed access device is illustrated in Fig. (**1**). The main components are a rectal tube, a compressed NiTi compression spring embedded in its front ring and connected to a moveable ring, and six expandable NiTi superelastic strips which are fixed using pin joints between the moveable ring and the distal ring of the rectal tube. At room temperature, the spring is in the retracted state with the strips straight. After introducing the access device into the rectum, its front end is attached to a support instrument outside the body. The spring maintains the retracted state. During the subsequent resistive heating procedure of the spring over its austenite transformation temperature range (A_s~A_f), it extends and generates a recovery stress to bend the strips, causing the rectum to expand. Upon cooling below M_s to M_f, the spring becomes less rigid and the curved strips push the spring back until they become straight again. As a result, the rectum returns to its normal state and the access device can be removed easily.

3. DESIGN CONSIDERATIONS

The accessible distance from the anal verge to the distal sigmoid colon for adult is about 200 mm [16], so the part of the access device in the rectum should also have this dimension and have a the same diameter (about 40 mm) as reported previously [5,8,10]. The distal ring (see Fig. **1**) is 30 mm long and the NiTi superelastic strips are 150 mm long (i.e. $L_{strip} = 150$ mm) with both ends fixed to the clamps. The moveable ring has an outer diameter of 34 mm (i.e. $D_{moveable} = 34$ mm) and an inner diameter of 24 mm. The clamps mounted on it are 5 mm wide (i.e. $L_{clamp} = 5$ mm).

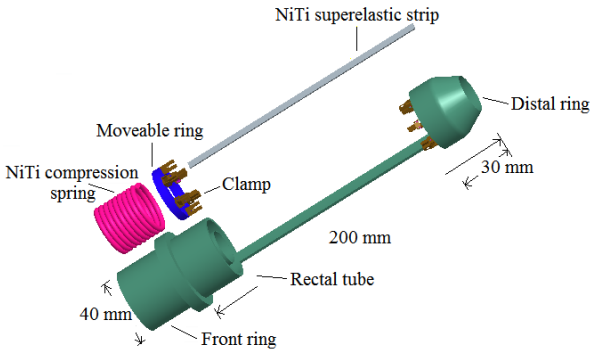

(**a**) Main components

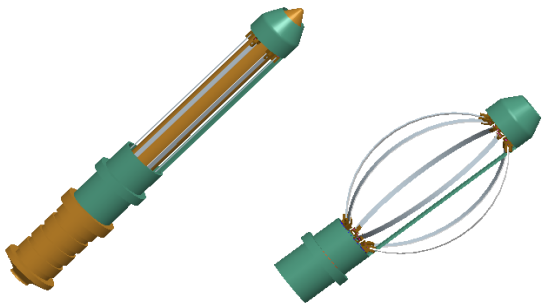

(**b**) Device in cold state (retracted) (**c**) Device in hot state (expanded)

Fig. (1). Structure of an access conceptual device based on NiTi compression spring and NiTi superelastic strips for gasless TEM.

In the hot state of the NiTi compression spring, the six NiTi superelastic strips are subject to an axial compressive force, which is generated by the spring during its shape recovery upon heating, and a lateral force from the expanded rectal wall. This causes the strips to undergo buckling. Usually, buckling should be avoided to ensure the stability of a structure, but here it is utilized to alter the geometry of the structure. The structural design considerations of this access device mainly lie in two aspects. One is to determine the dimensions of NiTi superelastic strips, such as thickness and breadth, so that it is strong enough to bear the resistance from the rectal wall, yet requires an applied axial compressive force (i.e. buckling force) that is as small as possible for a desired deflection. The other is to determine the parameters of the NiTi compression spring such as wire diameter, coil diameter and number of active turns, so that it is capable of yielding a sufficient force to bend the strips and accordingly realize the sufficient expansion of rectum. The design details of the rectal tube, the moveable ring and clamps are not presented here.

3.1. Transformation Temperatures

Since the shape control of the NiTi compression spring is performed in the surgical operating theatre by changing the temperature of the spring, all its transformation temperatures (i.e. M_s, M_f, A_s and A_f) must be higher than the local environmental temperature. Surgical operating theatres typically have a room temperature of about 20°C. In the case of M_f of about 25°C, A_f will be about 45°C due to the inherent hysteresis between martensitic transformation temperature and the reverse transformation temperature. The NiTi superelastic strips utilize the superelastic effect rather than the temperature dependent shape memory effect, so they should be in the austenite phase at all times, with an A_f below room temperature.

3.2. Dimensions of NiTi Superelastic Strips

According to the theory of buckling for slender columns under axial compression, the critical buckling force is smallest in the case of a pin-ended column [17]. Thus, in this design, the NiTi superelastic strips are pinned at both ends in order to minimize the force required to buckle them. Fig. (**2**) shows the geometry changes of the NiTi compression spring and those of a NiTi superelastic strip from the retracted to the expanded positions, where the lateral force acting on the strip by the expanded rectal wall is presumed to be a uniform load of intensity q along the strip and the compressive force from the spring ($F = F_{rec}/6$) acts with an eccentricity of $e = \dfrac{D_{moveable} - L_{clamp}}{2} = 14.5$ mm from the centroidal axis of the strip.

The elasticity of the rectal wall is usually quantified by rectal compliance, which is defined as the increase in volume per mmHg pressure. This is typically about 32 ml/mmHg in males and 24 ml/mmHg in females [18]. A constant maximum pressure of 20 mmHg (i.e. P_{co_2} =20 mmHg) is used to distend the rectum in the current gas insufflation TEM system, so the maximum volume of the rectum achieved in this

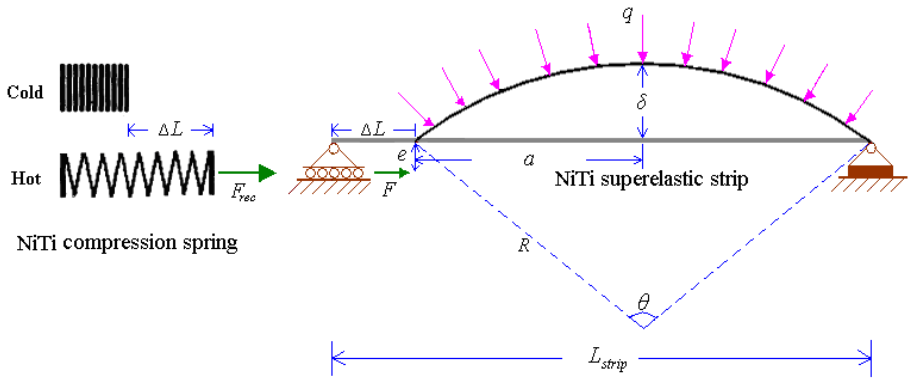

Fig. (2). Geometry changes of the NiTi compression spring and NiTi superelastic strip during the operation.

example case is 640ml. In order to avoid over-distension of the dilated rectum and potential tissue damage, the six curved superelastic strips should not be allowed to expand the rectum to exceed 640ml in volume. Taking the shape of the dilated rectum to be a standard ellipsoid, the half length of the major axis (a), the half length of the minor axis (δ) and the length of the strip (L_{strip}) can be expressed in terms of its angle in radians (θ) and radius of curvature (R) as follows:

$$a = R\sin(\frac{\theta}{2}) \tag{1}$$

$$\delta = R(1-\cos\frac{\theta}{2}) \tag{2}$$

$$L_{strip} = R\theta \tag{3}$$

The volume of the ellipsoid is given by

$$V = \frac{4\pi}{3}a\delta^2 + 2\pi ae^2 \tag{4}$$

By substituting $V = 640$ ml and $L_{strip} = 150$ mm into equations (1) to (4), the unknown variables can be calculated as $a = 66$ mm, $\delta = 31$ mm, $\Delta L = L_{strip} - 2a = 18$ mm. Then, the resistance from the rectal wall (F_{rectum}) can be approximately calculated from the following

Equations:

$$A_{rectum} = \pi^2 a\delta + 4\pi ae \tag{5}$$

$$F_{rectum} = P_{co_2} \cdot A_{rectum} \tag{6}$$

where A_{rectum} represents the surface area of the expanded rectum. Since the expanded rectum is supported by six NiTi superelastic strips, the lateral force acting on each strip (F_{strip}) and the corresponding load intensity are obtained as

$$F_{strip} = F_{rectum}/6 = 14.2 \text{ N},$$

$$q = F_{strip}/L_{strip} = 94.8 \text{ N/m}$$

The moment-curvature relationship [17], which is valid for the whole strip, is expressed as

$$EI\frac{d^2v}{dx^2} = -F(v+e) + \frac{qL}{2}x - \frac{q}{2}x^2 \tag{7}$$

where E denotes Young's modulus and has a value of $E = 83$ GPa for NiTi superelastic material, v denotes curvature at the point x along the strip and I denotes second moment of area. The expression for $v(x)$ can be obtained as

$$v(x) = A\sin(\sqrt{\frac{F}{EI}}x) + B\cos(\sqrt{\frac{F}{EI}}x) - \frac{q}{2F}x^2 + \frac{qL}{2F}x - e + \frac{EIq}{F^2} \tag{8}$$

which contains two constants of integration, namely

$$A = (e - \frac{EIq}{F^2})tg(\frac{L}{2}\sqrt{\frac{F}{EI}}) \tag{9}$$

$$B = e - \frac{EIq}{F^2} \tag{10}$$

The maximum deflection occurs at the middle of the strip (i.e. $x = \frac{L}{2}$) and is therefore given by

$$\delta = v(\frac{L}{2}) = (e - \frac{EIq}{F^2})[\sec(\frac{L}{2}\sqrt{\frac{F}{EI}}) - 1] + \frac{qL^2}{8F} \tag{11}$$

The strip collapses when this maximum deflection becomes infinite. According to the theory of column buckling for a pin-ended column [17], the lowest critical force (F_{cr}) at which this can occur is given by

$$\frac{L}{2}\sqrt{\frac{F_{cr}}{EI}} = \frac{\pi}{2} \tag{12}$$

from which

$$F_{cr} = \frac{\pi^2 EI}{L^2} \tag{13}$$

The compressive force to cause a desired maximum deflection of the strip should be less than this critical value. In other words, I and F should satisfy two conditions, i.e. $\delta(I,F) = 31$ mm and $F \in (0, F_{cr})$. Fig. (**3**) shows the theoretical variation of δ with F for strips of different second moment of area ($I = 0.1$ mm^4, 0.2 mm^4, …, 1.0 mm^4). It can be observed that, as F increases, δ increases in the negative direction for $I < 0.5$ mm^4, while it increases in the positive direction for $I \geq 0.5$ mm^4. This indicates that the strip with a second moment of area less than 0.5 mm^4 is too weak to withstand the lateral force and therefore sags as F increases

until it collapses, making it unsuitable for this application. A strip with a second moment of area above 0.5 mm^4 is strong enough to resist the lateral force and pushes the rectal wall outwards, so that the rectum can be expanded. Moreover, the higher the value of second moment of area, the greater the force required to achieve a desired deflection. So a strip with a smaller value of second moment of area is preferred. Therefore, a second moment of area $I = 0.5$ mm^4 is selected for this conceptual design.

For a NiTi superelastic strip with a rectangular cross section of thickness h and breadth b, its second moment of area is formulated as

$$I = \frac{bh^3}{12} \tag{14}$$

Let m be the ratio of breadth to thickness. The above equation can therefore be rewritten as

$$h = \sqrt[4]{\frac{12I}{m}} \tag{15}$$

By substituting a value of m and $I = 0.5$ mm^4 in equation (15), the thickness of the strip and in turn its breadth can be determined.

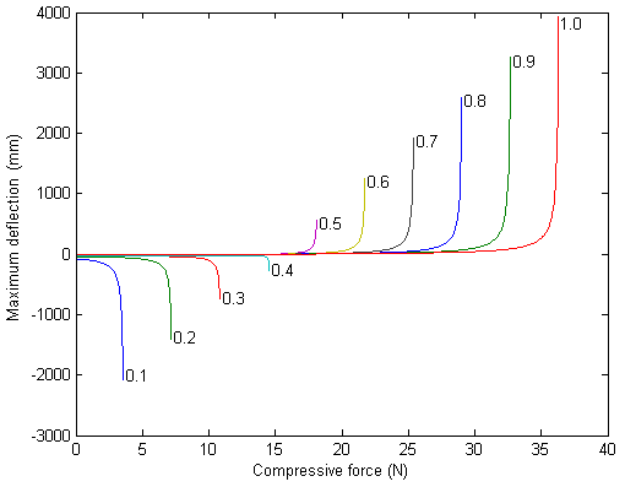

Fig. (3). Variation of maximum deflection (δ) with compressive force (F) for NiTi superelastic strips with different second moment of area (given in mm^4).

From Fig. (**4**), the force required to cause a convexity of 31mm for the selected NiTi superelastic strip is determined as $F = 17$ N. Then for six strips, it is $F_{rec} = 6F = 102$ N. This means that the total external load imposed on the NiTi compression spring is $F_{load} = F_{rec} = 102$ N.

3.3. Dimensions of NiTi Compression Spring

In linear elastic theory for conventional spring design (e.g. steel springs), the force produced by a spring at a given deflection depends linearly on the shear modulus (G) of its material. The NiTi spring is different from the conventional spring in that it exhibits a temperature dependent shear

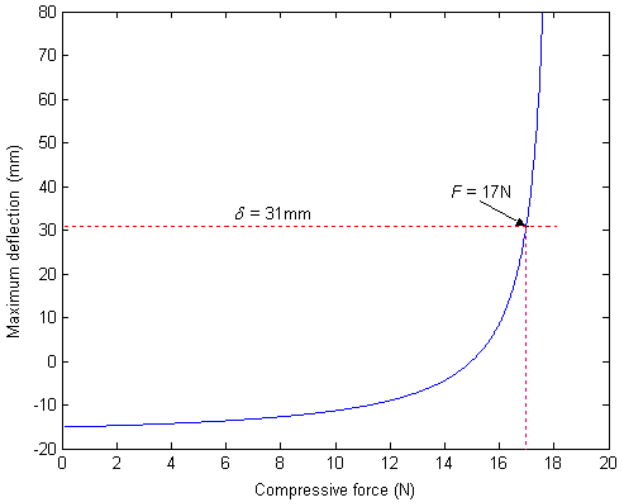

Fig. (4). The required compressive force (F) to achieve a desired maximum deflection (δ) of 31 mm for a strip with second moment of area of 0.5 mm^4.

modulus, which changes from high-temperature austenite phase to low-temperature martensite phase by approximately 300% [19]. Therefore, the relationship between applied load and deflection in both martensite and austenite must be considered when designing a NiTi spring.

The principal dimensions of the NiTi compression spring include wire diameter (d), mean coil diameter (D), number of active turns (n), length in the martensite phase (L_M) and shape set length, also called free length (L_f), which are related to the external load (F_{load}), stroke (ΔL), deflection in the martensite phase (δ_M) and deflection in the austenite phase (δ_A), as shown in Fig. (**5**). The fundamental formulas involved in the design are listed as below [20].

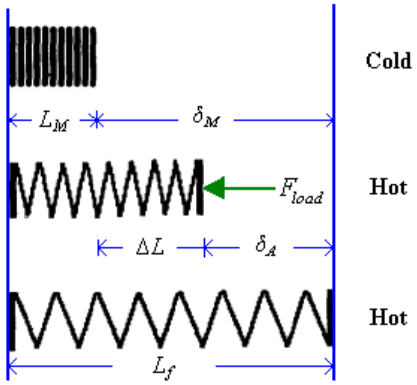

Fig. (5). Lengths and deflections of the NiTi compression spring.

The spring index is defined by

$$C = \frac{D}{d} \tag{16}$$

which usually has a value between 6 and 10 for practical applications.

The equation for maximum shear stress is

$$\tau_{\max} = \frac{8F_{load}Cw}{\pi d^2} \quad (17)$$

where w denotes stress correction factor and is calculated using Wahl's formula

$$w = \frac{4C-1}{4C-4} + \frac{0.615}{C} \quad (18)$$

The equation for the difference between shear strain in the austenite phase (γ_A) and maximum shear strain in the martensite phase ($\gamma_{\max}$) is:

$$\Delta\gamma = \frac{\Delta L d}{\pi n D^2} \quad (19)$$

The equation for spring rate is:

$$K = \frac{Gd^4}{8nD^3} \quad (20)$$

The main characteristic parameters for NiTi compression spring design are maximum shear stress ($\tau_{\max}$), maximum shear strain in the martensite phase ($\gamma_{\max}$), shear modulus in the austenite phase (G_A) and shear modulus in the martensite phase (G_M). Usually, in order to ensure a good fatigue property under cyclical loading, $\gamma_{\max}$ is constrained to 0.015 and $\tau_{\max}$ is kept to a relatively low value. As can be seen from equation (17), a lower value of $\tau_{\max}$ requires a wire with larger diameter for the spring, so more electrical power would be needed to actuate it. Therefore, $\tau_{\max}$ should be determined by a compromise among these factors. Here the design of the NiTi compression spring is considered in terms of a cyclic life of 1000 cycles, which is sufficient for this particular application. Increasing the cyclic life would require a larger diameter of wire, which in turn could require more heating current and would result in a slower cooling speed. Acceptable values of these design parameters are as follows:

$$\tau_{\max} = 200\,\text{MPa},\ \gamma_{\max} = 0.015,\ G_A = 23000\,\text{MPa},$$
$$G_M = 8000\,\text{MPa},\ C = 8$$

Then γ_A and $\Delta\gamma$ are calculated as

$$\gamma_A = \frac{\tau_{\max}}{G_A} = 0.0087, \qquad \Delta\gamma = \gamma_{\max} - \gamma_A = 0.0063$$

F_{load} and ΔL have been determined in the foregoing analysis as

$$F_{load} = 102\,\text{N}, \qquad \Delta L = 18\,\text{mm}$$

The wire diameter is first determined using equation (17) as $d = 3.5$ mm, the mean coil diameter is obtained from equation (16) as $D = 28$ mm and the numbe

r of active turns is found from equation (19) to be $n = 4$. The total number of coils including two end hooks is given by:

$$N = n + 2 = 6$$

The spring rate in the austenite phase is given by equation (20) as

$$K_A = 4.86\ \text{KN/m}$$

Accordingly, the deflections in the austenite phase and in the martensite phase are

$$\delta_A = \frac{F_{load}}{K_A} = 21\ \text{mm}, \quad \delta_M = \delta_A + \Delta L = 39\ \text{mm}$$

Finally, the fully compressed length of NiTi SMA spring in the martensite phase (L_M) and its shape set length are determined as

$$L_M = dN = 21\ \text{mm}, \quad L_f = L_M + \delta_M = 60\ \text{mm}$$

3.4. Response Time of NiTi Compression Spring

Resistive heating and cooling under natural convection is the most convenient way to excite NiTi SMA actuators and as such is commonly used in practice. A complete actuation cycle of the NiTi SMA actuator involves heating and cooling it through its transformation temperature region ($M_f \sim A_f$). Its overall response time consists of the actuation time upon heating and resetting time upon cooling. The heating time (t_h) in seconds for a NiTi SMA wire electrically heated by direct current, with convection between its surfaces and the surrounding air being the major source of heat loss, and the cooling time (t_c) through natural convection can be estimated by the following simplified equations [18]:

$$t_h = J_h \ln\left(\frac{T_{\max} - T_a}{T_{\max} - T_h}\right) + 121.23\frac{d^4}{I^2}\left(\frac{T_{\max} - T_a}{T_{\max} - A_f}\right) \quad (21)$$

$$t_c = J_c\left[\ln\left(\frac{T_h - T_a}{T_c - T_a}\right) + \frac{28.88}{M_s - T_a}\right] \quad (22)$$

where $T_{\max}$ is maximum achievable temperature (°C) in the NiTi SMA wire by an electrical current after prolonged heating, T_a is ambient temperature, T_h is target temperature upon heating and initial temperature upon cooling, T_c is target temperature upon cooling, J_h is time constant for heating, J_c is the time constant for cooling, d is wire diameter (mm) and I is electrical current (A). During the heating procedure, when the rate of heat generated by the electrical current is equal to the rate of heat loss by convection, the wire temperature will approach $T_{\max}$. The value of $T_{\max}$ depends on electrical current, wire diameter and also the convection conditions in the surroundings, which could be natural convection or forced air cooling. By setting

$T_h = A_f$ and $T_c = M_f$, the heating time coincides with actuation time and the cooling time is equivalent to the resetting time for the NiTi SMA wire. Empirical measurements have shown that for heating in sill air, J_h, $T_{\max}$ and J_c can by given by the following expressions [20]:

$$J_h = 12.06 + 12.418d^2 \tag{23}$$

$$T_{\max} = 16.383\frac{I}{d} + 3.987\frac{I^2}{d^2} \tag{24}$$

$$J_c = 13.25 + 18.7063d^2 \tag{25}$$

Substituting the expression for $T_{\max}$ into equation (21) yields the following expression of t_h in terms of I and d:

$$t_h = J_h \ln\left(\frac{16.383\frac{I}{d} + 3.987\frac{I^2}{d^2} - T_a}{16.383\frac{I}{d} + 3.987\frac{I^2}{d^2} - T_h}\right) + 121.23\frac{d^4}{I^2}\left(\frac{16.383\frac{I}{d} + 3.987\frac{I^2}{d^2} - T_a}{16.383\frac{I}{d} + 3.987\frac{I^2}{d^2} - A_f}\right) \tag{26}$$

By applying the wire diameter of the specified NiTi compresion spring (d = 3.5 mm) to equation (24) and setting $T_{\max}$ = A_f, the minimum current required to heat it from room temperature ($T_a = 20$ °C) to A_f can be found to be 6.6A. As shown in Fig. (**6**), the actuation time is highly dependent upon the amount of current used. If the desired actuation time is 60 s, the required current can be determined graphically as 22.3 A. Assuming M_s to be 10°C above M_f and setting $T_h = A_f$, $M_f = T_c$, the resetting time under natural convection is obtained from equation (22) as about 856.8 s.

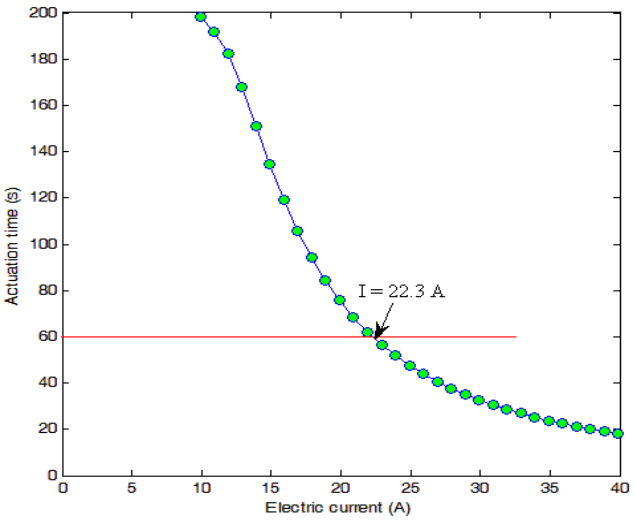

Fig. (6). Actuation time (t_h) vs. electric current (I) curve for NiTi TWSMA wire obtained from equation (26).

4. DISCUSSION

An access device using combined shape memory effect and superelastic technologies avoids the risks caused by CO_2 gas insufflation and, with careful operational design, it could also facilitate surgeons to perform TEM. The NiTi compression spring is hollow for surgical instruments to pass through and allows easier exchange as well as more flexible manipulation of the surgical instruments. It also contributes to a lightweight and compact device. These advantages are not available with other alternative actuators, such as those driven by a motor.

A precondition to realizing the design of this new access device is to obtain NiTi SMA material, i.e. suitable NiTi compression spring and NiTi superelastic strips, with properties that meet the application requirements summarized in Table **1**. At present, NiTi SMA material is mainly supplied in the cold-drawn state in the form of round wire, tube or rectangular section strip, while a few companies also provide small NiTi springs with wire diameter less than 1 mm. The specified NiTi wire and strip can readily been obtained and made into the desired compression spring and superelastic strips through simple heat treatment processes. As far as the safety of this access device is concerned, non-contact between the NiTi compression spring and the rectum eliminates the worry about thermal damage of rectal tissues by the electrically heated NiTi compression spring and the need for extra insulation. Moreover, the NiTi superelastic strips can be wrapped with a material such as silicone to avoid any snaring of rectal tissues by their rims.

A potential problem for consideration is the response speed of the device, which is dictated by the actuation speed and the resetting speed of NiTi SMA actuators involved. The rapid actuation upon heating can be easily achieved by increasing the electrical current passing through the NiTi compression spring, although a very high-current power source is required. Improving the resistive heating efficiency in some way would help to lower the current needed to satisfy the requirement for rapid actuation. The topic is under investigation. The rather slow resetting procedure upon cooling under natural convection is not acceptable and needs to be improved by forced cooling. The usual approach is to design special cooling conduits such as a channel of flowing water surrounding the NiTi compression spring. A simpler and space-saving method is to use NiTi tubes rather than NiTi wires to construct NiTi compression spring, so that the spring acts as its own cooling conduit.

5. CONCLUSIONS

The conceptual theoretical design for a novel access device to be used in TEM is presented, which takes advantage of the temperature dependent actuation mechanism and superelasticity of NiTi SMA material for use in a device for

Table 1. The Specifications of NiTi SMA Components in the Design of the New Access Device

NiTi SMA Material	NiTi Compression Spring	NiTi Superelastic Strips
Transformation temperatures	$M_f \approx 25^oC$ $A_f \approx 45^oC$	$A_f < 20^oC$
Size of cross section	Diameter =3.5 mm	Second moment of area = 0.5 mm^4
Shape	Spring set length = 60 mm Total number of coils = 6 Mean spring diameter = 28 mm	Straight line Length = 150 mm

gasless dilation of the rectum. It has potential advantages over the existing counterparts. The main design issues for the NiTi compression spring and NiTi superelastic strips have been considered and indicate the practical feasibility of these components. Based on the theoretical design, a prototype device is under development and will be evaluated in terms of performance characteristics to verify the design procedure in the next stage.

REFERENCES

[1] Peerbooms JC, Simons JL, Tetteroo GWM, De Graaf EJR. Curative resection of rectal cancinoid tumors with transanal endoscopic microsurgery. J Laparoendosc Adv Surg Tech A 2006; 16: 435-8.

[2] Zacharakis E, Freilich S, Rekhraj S, *et al*. Transanal endoscopic microsurgery for rectal tumors: the St. Mary's experience. Am J Surg 2007; 194: 694-8.

[3] Darwood RJ, Wheeler JMD, Borley NR. Transanal endoscopic microsurgery is a safe and reliable technique even for complex rectal lesions. Br J Surg 2008; 95: 915-8.

[4] Wan WH, Lee J, Clarke MJ, Cheng A. Transanal endoscopic microsurgery. ANZ J Surg 2009; 79: 294-5.

[5] Buess G, Mentges B, Manncke K, Starlinger M, Becker HD. Technique and results of transanal endoscopic microsurgery in early rectal cancer. Am J Surg 1992; 163: 63-70.

[6] Winde G, Nottberg H, Keller R, Schmid KW, Bunte H. Surgical cure for early rectal cancinomas (T1): transanal endoscopic microsurgery vs. anterior resection. Dis Colon Rectum 1996; 39: 969-76.

[7] Cuschieri A. Technology for minimal access surgery. BMJ 1999; 319: 1304-9.

[8] Nakagoe T, Ishikawa H, Sawai T, Tsuji T, Tanaka K, Ayabe H. Surgical technique and outcome of gasless video endoscopic transanal rectal tumour excision. Br J Surg 2002; 89: 769-74.

[9] Nakagoe T, Ishikawa H, Sawai T, *et al*. Gasless, video endoscopic transanal excision for carcinoid and laterally spreading tumors of the rectum. Surg Endosc 2003; 17(8): 1298-304.

[10] Kanehira E, Yamashita Y, Omura K, Kinoshita T, Kawakami K, Watanabe G. Early clinical results of endorectal surgery using a newly designed rectal tube with a side window. Surg Endosc 2002; 16: 14-7.

[11] Yamashita Y, Sakai T, Maekawa T, Shirakusa T. Clinical use of a front lifting hood rectoscope tube for transanal endoscopic microsurgery. Surg Endosc 1998; 12: 151-3.

[12] Luo H, Abel EW, Hewit JR, Slade AP, Steele RJ. Development of a two-way shape memory actuator for transanal endoscopic surgery. In: Hamza MH, Ed. Proceedings of IASTED international conference on Applied Simulation and Modelling; Marbella: ACTA Press 2003; pp. 573-77.

[13] Wang Z, Hewit J, Abel E, Slade A, Steele B. Development of A Shape Memory Alloy Actuator for Transanal Endoscopic Microsurgery. In: Wang WQ, Ed. Proceedings of the 2005 IEEE Engineering in Medicine and Biology 27th Annual Conference; Shanghai: IEEE Press 2006; pp. 4341-44.

[14] Friend CM, Morgan NB. Medical Applications for Shape Memory Alloys (SMA). Suffolk: Professional Engineering Publishing Limited 1999.

[15] Tarnita D, Tarnita DN, Bizdoaca N, Mindrila I, Vasilescu M. Properties and medical applications of shape memory alloys. Rom J Morphol Embryol 2009; 50: 15-21.

[16] Van Dalen RM, Hershman MJ. How to do it in surgery: transanal endoscopic microsurgery. Br J Hosp Med 1997; 58(10): 498-500.

[17] Gere JM, Timoshenko SP. Mechanics of Materials. London: Chapman & Hall 2000.

[18] Sloots CEJ, Felt-Bersma RJF, Cuesta MA, Meuwissen SGM. Rectal visceral sensitivity in healthy volunteers: influences of gender, age and methods. Neurogastroenterol Motil 2000; 12: 361-8.

[19] Otsuka K, Wayman CM, Eds. Shape Memory Materials. Cambridge: Cambridge University Press 1998.

[20] Waram TC. Actuator design using shape memory alloys. Ontario: Waram TC 1993.

Received: May 30, 2009 Revised: June 11, 2009 Accepted: June 12, 2009